Generation of a Family of Protein Fragments for Structure–Folding Studies. 1. Folding Complementation of Two Fragments of Chymotrypsin Inhibitor-2 Formed by Cleavage at Its Unique Methionine Residue

Gonzalo de Prat Gay and Alan R. Fersht*

MRC Unit for Protein Function and Design, Department of Chemistry, Cambridge University, Lensfield Road, Cambridge CB2 1EW, U.K.

Received February 21, 1994; Revised Manuscript Received April 19, 1994®

ABSTRACT: The suitability of the barley chymotrypsin inhibitor-2 for study by fragmentation and complementation has been analyzed. The primary residue for binding to proteases, Met-59 (the unique methionine in the sequence), lies in a broad, solvent-exposed loop. The bond between Met-59 and Glu-60 was cleaved by cyanogen bromide. The two fragments thus obtained, i.e., CI-2(20–59) and CI-2(60–83), associate (K_D = 42 nM) to yield a complex that has fluorescence and circular dichroism spectra identical to those of uncleaved chymotrypsin inhibitor-2. Recovery of native-like structure is further indicated by the ability of the complex to inhibit chymotrypsin, although the $[I]_{50\%}$ is 140-fold higher than for the uncleaved inhibitor. CI-2(60–83) appears to be highly disordered in water, but fragment CI(20–59) forms significative structure, as judged by its circular dichroism spectra and evidence from one-dimensional NMR. The circular dichroism spectra of CI-2(20–59) approach the baseline in 4 M guanidinium chloride but display characteristics of an α-helix in the presence of trifluoroethanol. Analytical ultracentrifugation shows no concentration-dependent change in the molecular weight of the monomer of CI-2(20–59) . Both one- and two-dimensional NMR of the complex [CI-2(20–59)·(60–83)] show unequivocally the presence of a folded structure, which appears to be slightly different from the uncleaved native protein.

The understanding of how proteins function and the design of such molecules with novel biological activities depend on understanding how proteins fold to their tertiary structure. One approach to tackling the problem is to dissect a protein into smaller fragments and analyze their structures individually or combine them for folding complementation. Initially, it was believed that short fragments in solution formed secondary structure only in the presence of other segments of the protein through stabilizing tertiary interactions (Anfinsen & Scheraga, 1975). The C-peptide of RNase A was shown to form a marginally stable α-helix in water (Brown & Klee, 1971); since then, a wealth of information has been obtained on peptide structure in solution [for a review, see Dyson and Wright (1991)]. The complementation of peptide fragments in staphylococcal nuclease, barnase, and adenylate kinase has been described (Taniuchi & Anfinsen, 1971; Hartley, 1977; Saint Girons *et al.*, 1987; Sancho & Fersht, 1992); fragments of BPTI were S–S linked to obtain a structured folding intermediate (Oas & Kim, 1988), and isoleucyl-tRNA synthetase fragments have been assembled after a random cleavage (Shiba & Schimmel, 1992). Peptide fragments of the dimeric Trp repressor were also described to associate into a functional complex (Tasayco & Carey, 1992).

In the present study, we examine a truncated (residues 20–83) form of the chymotrypsin inhibitor-2 (CI-2), a small (M_r 7303) monomeric protein from barley seeds (Svendsen et al., 1980), which has been cloned in *Escherichia coli* (Longstaff *et al.*, 1990), and its crystal (McPhalen & James, 1987; Harpaz *et al.*, 1994) and NMR solution structures have been refined (Clore *et al.*, 1987; Ludvigsen *et al.*, 1991). The first 19 residues are unstructured and do not contribute to the stability (McPhalen & James, 1987; Ludvigsen *et al.*, 1991; Jackson & Fersht, 1991; Jackson *et al.*, 1993). CI-2 unfolding follows a simple two-state reversible transition for both equilibrium and kinetics (Jackson & Fersht, 1991). The inhibitor has a broad loop which contains the reactive site bond, Met-59–Glu-60. The bond is not usually cleaved by the protease, but cleavage may be induced by certain mutations (Longstaff *et al.*, 1990). This bond is also a potential site for chemical cleavage using cyanogen bromide (Gross & Witkop, 1961). In the present paper we cleaved and isolated two CI-2 fragments, CI-2(20–59) and CI-2(60–83), and we describe their association to give a structure similar to that of the folded uncleaved protein.

We have chosen to cleave the protein at this position not as an isolated study on a particular pair of peptides but as a prelude to an extensive investigation. The presence of a single methionine at position 59 is common to virtually all the large number of mutants of CI-2 being made in this laboratory, and so a large number of mutant fragments may be generated for future studies of structure–folding relationships.

MATERIALS AND METHODS

Chemicals. Cyanogen bromide (CNBr) and trifluoroethanol (TFE) were purchased from Fluka, Switzerland. Guanidinium chloride (Gdm·Cl) was sequanal grade from Pierce, Rockford, IL. DE-52 resin was obtained from Whatman, Maidstone, England. IPTG was from HT Biotechnology, England, and succinyl-Ala-Pro-Phe *p*-nitroanilide was from Sigma, St. Louis, MO). All other reagents were of analytical grade, and water was deionized and purified on an Elgastat system.

Purification of CI-2. A truncated form of CI-2 comprising residues 20–83 was cloned into a pTZ18U-based vector (Pharmacia, Uppsala, Sweden) under the control of the coupled T7 RNA polymerase/ϕ10 promoter system, resulting in a high-expression vector, pCI-2 (M. Rheinnecker, unpub-

* To whom correspondence should be addressed.

® Abstract published in *Advance ACS Abstracts,* June 1, 1994.

0006-2960/94/0433-7957$04.50/0

lished; Jackson *et al.*, 1993). The plasmid was transformed into TG2 *E. coli* cells, and the cells were grown in 2XTY medium to A_{600} = 1.0; the expression was induced by adding IPTG to 0.4 mM. After overnight incubation at 37 °C, the cells were spun down and sonicated in 50 mM sodium phosphate buffer, pH 6.5, with 5 mM 2-mercaptoethanol and addition of 10 μg/mL DNase. The supernatant was quickly heated to 55 °C, incubated for 30 min, cooled, and cleared by centrifugation. Ten grams of preswollen DE-52 was added per liter of culture. The suspension was incubated for 15 min and vacuum filtered to remove the resin with bound impurities. The filtrate was subjected to ammonium sulfate precipitation between 35 and 90%. The precipitate from 90% ammonium sulfate was resuspended in water and dialyzed against water until the absorbance at 260 nm of the dialysis buffer remained unchanged. The sample, which was ≥80% pure, was concentrated by lyophilization, resuspended in 50 mM Bis-Tris·HCl, pH 7.0, and 0.3 M NaCl, loaded into a preparative Superdex 75 gel filtration column (Pharmacia), and eluted with the same buffer. The main peak was dialyzed against water, lyophilized, and stored as a powder at −20 °C, with a final yield of 90 mg/(liter of culture). The M_r was determined by electron spray ionization mass spectrometry (ESI) to be 7303.

Cleavage and Purification of the Fragments. Thirty milligrams of CI-2 was dissolved in 30 mL of water, and the pH was taken to 2.3 with HCl. The mixture was incubated for 20 min at 25 °C, and 60 mg of CNBr was added. After 5 h, the sample was diluted 1:4 in water and the CNBr was partly removed by rotary evaporation. The sample was then lyophilized, dissolved in 5% acetonitrile and 0.1% TFA, and purified by reversed-phase HPLC, using a C8 Dynamax 300A (Rainin) column and a linear gradient of 20 to 50% acetonitrile in 0.1% TFA. Two fragments were obtained, CI-2(20–59) and CI-2(60–83); the molecular weights were measured by ESI to be 4401 for CI-2(20–59) and 2871 for CI-2(60–83), in excellent agreement with the molecular weights calculated from the primary sequence. Amino acid analysis corroborated the identity of the fragments and indicated that only one Met residue for CI-2(20–59), corresponding to the first uncleaved (ATG) residue, Met-59, was presumably converted into homoserine as a result of the CNBr cleavage reaction.

The concentration of the fragments was calculated using tabulated molar extinction coefficients for tryptophan and tyrosine in model compounds (Gill & von Hippel, 1989); CI-2(20–59) contains one Trp residue, whereas CI-2(60–83) has only one Tyr residue.

Fluorescence. Fluorescence spectra and single measurements were recorded on an LS-5B Perkin-Elmer luminescence spectrometer under the conditions described in the figures. Gdm·Cl equilibrium denaturation was performed in 50 mM sodium phosphate buffer, pH 6.3 (7.75 mM NaH_2PO_4, 2.25 mM Na_2HPO_4). The temperature in all experiments was 25.0 ± 0.1 °C unless otherwise stated.

^{1}H-NMR Spectra. ^{1}H-NMR spectra were recorded on a Bruker AMX-500 spectrometer equipped with an X32 computer. Samples were prepared by dissolving lyophilized fragments in 90% H_2O/10% ^2H_2O in 50 mM phosphate buffer, pH 6.3, for 1D spectra and 50 mM sodium acetate buffer, pH 4.5, for 2D spectra. Two-dimensional nuclear Overhauser enhancement spectra (NOESY) were acquired at 5 °C with a mixing time of 150 ms, using time-proportional phase increments. The spectra were recorded with 4096 t_2 data points and 512 t_1 increments, with a spectral width of 8064 Hz in both dimensions.

Circular Dichroism. CD spectra were obtained with a Jasco J720 instrument, using 0.05-cm path cuvettes. The spectra were the average of 10 scans at 20 nm/min, and the buffer baselines were subtracted. We analyzed the far-UV region from 250 down to 180 nm in order to obtain reliable data (Johnson, 1990). For the dependence of the ellipticity change of CI-2(20–59) on concentration, a 1-cm path cuvette was used, and 12 scans from 255 to 185 nm were recorded at each fragment concentration, including a buffer baseline. An average value was obtained between 220 and 221 nm, and this was plotted against concentration (see below). The thermal denaturation of the [CI-2(20–59)·(60–83)] complex was monitored at 200 nm where the signal to noise ratio is optimal. The data were fitted to obtain the temperature midpoint of the transition, T_m.

Calculation of Binding and Rate Constants for Fragment Reassociation. Increasing amounts of CI-2(60–83) were added to a solution of a fixed concentration of CI-2(20–59) in 10 mM phosphate buffer, pH 6.3 (7.75 mM NaH_2PO_4, 2.25 mM Na_2HPO_4), and the fluorescence was measured after a 2-h incubation at 25 °C, with excitation at 280 nm and emission at 356 nm. The experiment was carried out in siliconized glass tubes and fluorescence cuvettes in order to minimize binding of the peptides to the glass. The fluorescence values of a blank solution containing only CI-2(60–83) at each of the concentrations was subtracted for each point, although the fluorescence of CI-2(60–83) is low since it has no Trp residues. The dissociation constant of the complex was calculated by fitting the plot of the observed fluorescence change of CI-2(20–59) versus added CI-2(60–83) to the following equation assuming a 1:1 stoichiometry:

$$F_{measd} = 0.5\Delta F_{int}([W]_0 + [Y]_0 + K_D - [(([W]_0 + [Y]_0 + K_D)^2 - 4[W]_0[Y]_0)]^{0.5}) \quad (1)$$

where $[W]_0$ is the total concentration of CI-2(20–59), which is held constant, $[Y]_0$ is the variable total concentration of CI-2(60–83), ΔF_{int} is the difference of intrinsic fluorescence between the free and complexed fragments, and K_D is the dissociation constant.

Analytical Ultracentrifugation. Five samples of CI-2(20–59) with A_{280} from 0.1 to 0.5 in 10 mM phosphate buffer, pH 6.3 (7.75 mM NaH_2PO_4, 2.25 mM Na_2HPO_4), and one buffer blank were set up for the experiment. Sedimentation equilibrium measurements were made using a Beckman An-G analytical rotor in a Beckman L8-70 ultracentrifuge with a Prep ultraviolet scanner, interfaced to an Apple III microcomputer [for details, see Butler and Kühlbrandt (1988)]. The samples were centrifuged to equilibrium at 45 000 rpm at 20 °C. Scans were taken at intervals of 24 h; the first successive scan without change with respect to the previous was taken to be at equilibrium.

Apparent weight-average molecular mass ($\bar{M}_{W,app}$) was determined using the following equation:

$$\bar{M}_{W,app} = [d \ln(c_2)/dr^2]2RT/\omega^2(1 - \phi'\rho_0) \quad (2)$$

A plot of $\bar{M}_{W,app}$ was obtained against the concentration along the cell. For a detailed explanation of the terms and method, refer to Casassa and Eisenberg (1964).

RESULTS

CI-2 was cleaved at the reactive site bond Met-59–Glu-60 using CNBr to the fragments of Figure 1, in which the secondary structure in full wild-type protein is indicated, based on the information of the refined NMR solution structure

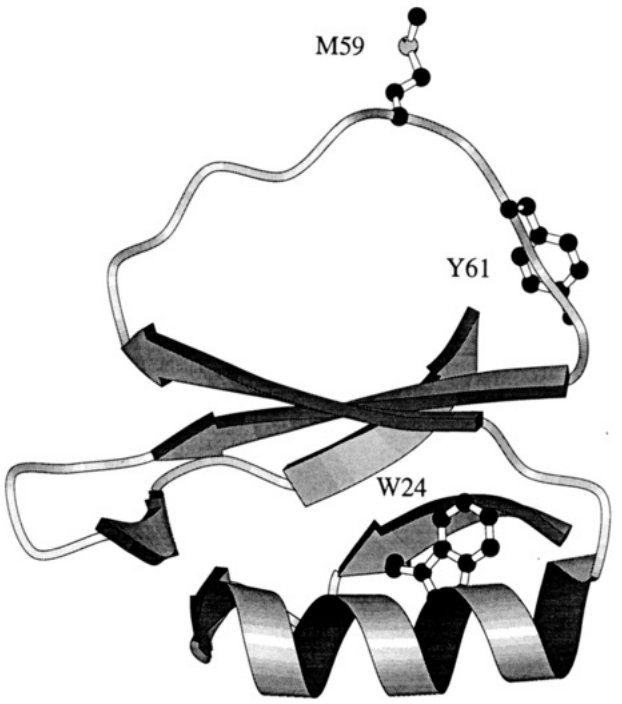

FIGURE 1: Ribbon diagram of CI-2 showing key residues in this study. The picture was produced using the program Molscript, based on information of the NMR structure (Ludvigsen *et al.*, 1991).

(Ludvigsen *et al.*, 1991). Figure 1 shows a ribbon diagram of CI-2 indicating the residues W24, M59, and Y61. W24 is buried in the hydrophobic core, and Y61 is at one side of the loop, relatively exposed; M59 is highly exposed to the solvent, accessible to the CNBr.

Fluorescence Spectra for Formation of the [CI-2(20–59)·CI-2(60–83)] Complex and Determination of the Binding Constant. CI-2 contains only one Trp residue, which is buried in the native structure (McPhalen & James, 1987). However, upon unfolding it is exposed to the solution, and the fluorescence emission increases with a maximum at 356 nm (Jackson & Fersht, 1991). Fragment CI-2(20–59) contains that Trp residue, so it is possible to probe refolding when combined with CI-2(60–83), which contains no major fluorescent residue. CI-2(20–59) was held at a fixed concentration and mixed with increasing concentrations of CI-2(60–83) (Figure 2). The fluorescence decreases as the concentration of CI-2(60–83) is increased, and the final spectrum is identical to that of folded native CI-2 (not shown).

The value of K_D obtained at 0.5 μM CI-2(20–59) is 42 ± 20 nM (Figure 3). At 1 μM, the fluorescence change titrates at 1:1 concentration, verifying equimolar stoichiometry of binding, but making the determination of K_D inaccurate (not shown). Concentrations lower than 0.5 μM could not be analyzed reliably because of the limitations of the technique.

Stability of the [CI-2(20–59)·(60–83)] Complex. Effect of pH, Guanidinium Chloride, and Temperature. The effects of pH, temperature, and chemical denaturation on the complex were analyzed. Figure 4a shows the effect of pH from 2.0 to 9.0 on the equilibrium of complex formation. Below pH 3.0, the complex is dissociated, and above pH 4.5, it is stable at the concentration of 5 μM. When the [CI-2(20–59)·(60–83)] complex (1:1 ratio) was treated with increasing concentrations of Gdm·Cl, a single denaturation transition with a midpoint of 1.0 M was obtained at 5 μM concentration (Figure 4b). This transition seems to be monitoring the dissociation/unfolding of the complex. CI-2(20–59) alone does not display a cooperative transition with Gdm·Cl monitored by fluorescence (not shown).

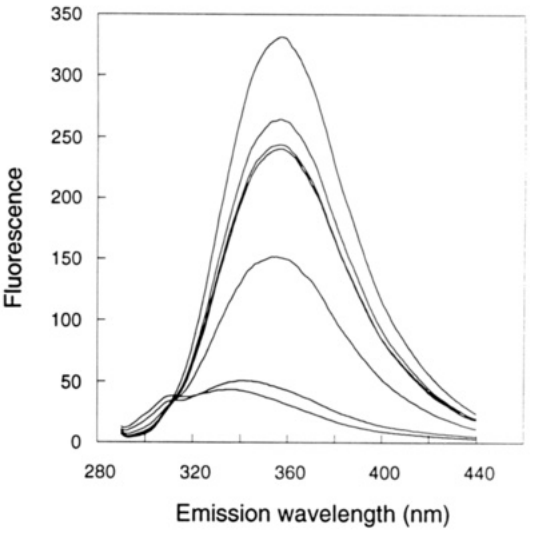

FIGURE 2: Change in the fluorescence spectrum of CI-2(20–59) (5 μM) upon addition of 0.5–5 μM CI-2(60–83). The decrease in fluorescence at 356 nm is approximately 7-fold. Excitation wavelength is at 280 nm, and the buffer is phosphate, pH 6.3.

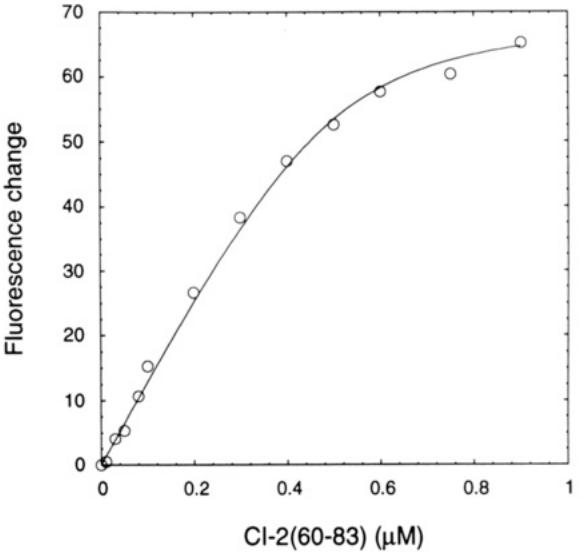

FIGURE 3: Equilibrium association of CI-2(20–59) and CI-2(60–83) followed by the change in fluorescence at 356 nm. The fragment at constant concentration, CI-2(20–59), is at 0.5 μM. The fluorescence of CI-2(60–83) was subtracted from each point. The reactions were carried out in 1-mL volumes in 10 mM phosphate buffer, pH 6.3, equilibrated for 2 h at 25 °C. The solid line was calculated using eq 1. K_{diss} = 42 nM.

The effect of the temperature on the [CI-2(20–59)·(60–83)] complex was monitored by the change in ellipticity at 200 nm (Figure 4c). The T_m of the complex denaturation should be dependent on the fragment concentration; there is an apparent T_m of 48 ± 0.4 °C at a fixed concentration of 5 μM complex. The individual fragments do not show a significant cooperative transition (G. de Prat Gay, unpublished).

Secondary Structure of the Isolated Fragments and of the Complex, Monitored by Circular Dichroism. Molar Ellipticity Change upon Addition of CI-2(60–83) to CI-2(20–59). The far-UV circular dichroism spectrum of the CI-2(60–83) fragment in Figure 5a is indicative of disordered structure with a minimum at 200 nm; the same spectrum in 5 M Gdm·Cl does not differ (not shown). However, the CD spectrum of CI-2(20–59) also has a minimum at 200 nm but shows a shoulder at 212 nm and is clearly different from the spectrum in 5 M Gdm·Cl (Figure 5b), which suggests the presence of residual structure. When native CI-2 was analyzed under

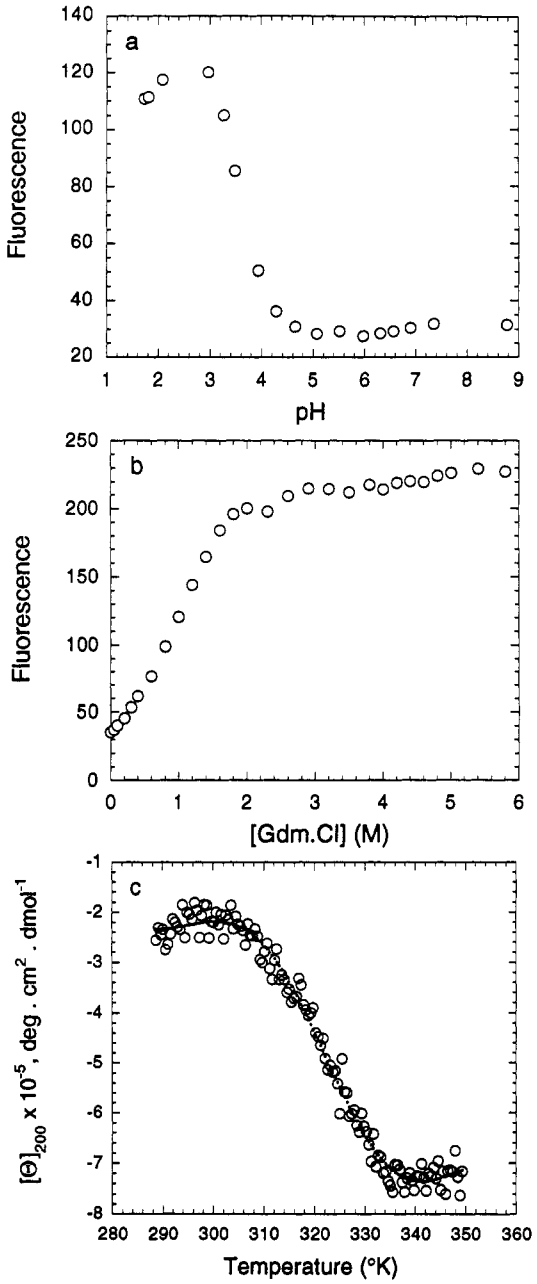

FIGURE 4: Stability of the [CI-2(20–59)·(60–83)] complex. (a) 5 μM complex was incubated for 2 h at the different pHs, using citrate–phosphate buffers. (b) 5 μM complex (25 mM phosphate, pH 6.3) was preequilibrated for 1 h at 25 °C, mixed with Gdm·Cl, and then incubated for another hour before the fluorescence was measured. (c) 5 μM complex (10 mM phosphate, pH 6.3) was incubated for 1 h before thermodenaturation measured by $\Delta[\Theta]_{200nm}$. Scan rate was 50 °C/h, in 0.2 °C intervals. The apparent T_m (48 ± 0.4 °C) is the midpoint of the transition.

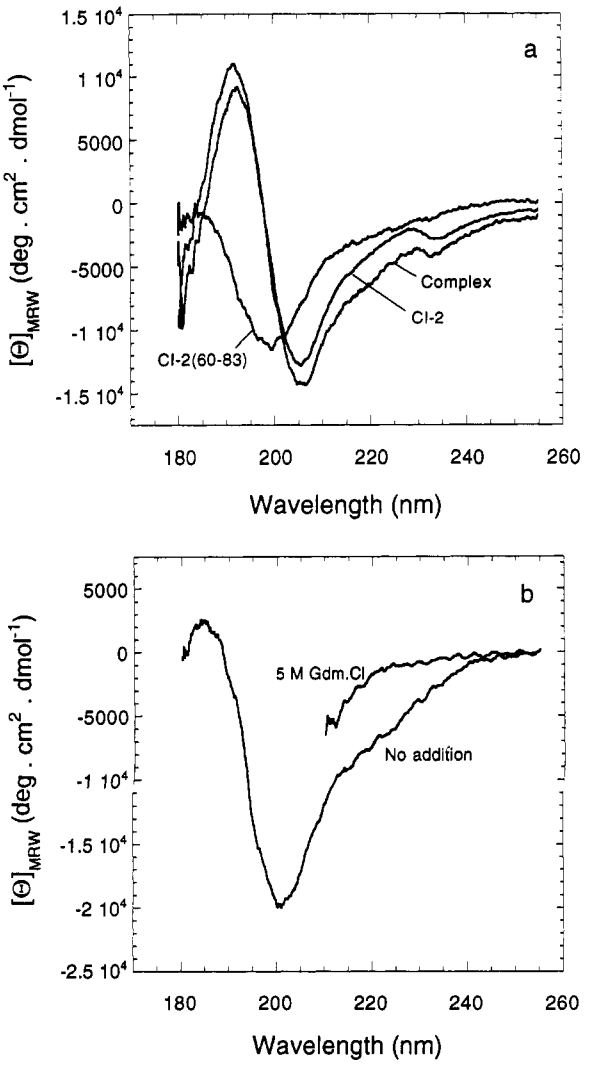

FIGURE 5: (a) CD spectra of CI-2(60–83), [CI-2(20–59)·(60–83)], and uncleaved CI-2. Concentration of each component is 20 μM in 10 mM phosphate, pH 6.3, in a 0.05-cm path length cuvette. Twelve scans at 25 °C were averaged. (b) CD spectra of CI-2(20–59) in 10 mM phosphate buffer and 5 M Gdm·Cl in the same buffer.

the same conditions, the spectrum seemed to be a combination of the features of an α-helix/β-sheet-containing protein, namely, a positive band at 190 nm, a minimum at 205 nm, a shoulder at 215 nm, and a negative band at 233 nm presumably attributable to Trp-24 (Figure 5a). Since the protein contains 20% α-helix and 45% β-sheet, the region of 210–220 nm will not be characteristic of a particular secondary structure element, making it difficult to assign unequivocally all of the bands of the spectrum. A spectrum identical to that of the native uncleaved CI-2 is obtained after the mixing of the two fragments in equimolar ratio, supporting the recovery in the [CI-2(20–59)·(60–83)] complex of all of the secondary structure of the uncleaved CI-2 (Figure 5a).

In order to observe the gradual recovery of secondary structure of the complex, a difference CD spectrum was determined for the formation of the complex upon addition of increasing amounts of CI-2(60–83) to CI-2(20–59). The change in the spectrum (Figure 6a) is dominated by the increase in ellipticity at 193 nm from α-helix formation; minor observable changes occur at 213 and 233 nm, which are likely to result from β-strand formation and from changes in the environment of Trp-24, respectively. The major change in molar ellipticity takes place at 193 nm and is plotted in Figure 6b against the concentration; a tight binding is evident with a stoichiometry of 1:1 as observed in fluorescence.

Monomeric State of CI-2(20–59). CI-2(20–59) has a considerable number of exposed hydrophobic side chains, in particular in the region from 45 to 59, with several residues participating in the hydrophobic core in the native uncleaved CI-2 (McPhalen & James, 1987; Jackson *et al.*, 1993). A peptide comprising residues 45–59 has been synthesized and found to be highly insoluble (G. de Prat Gay, unpublished); however, CI-2(20–59) includes this region and remains in solution. We considered the possibility that CI-2(20–59) forms an oligomer to overcome the side-chain insolubility. To test this, we performed an analytical centrifugation experiment. A plot of the apparent weight-average molecular mass versus fragment concentration indicates that CI-2(20–59) is a

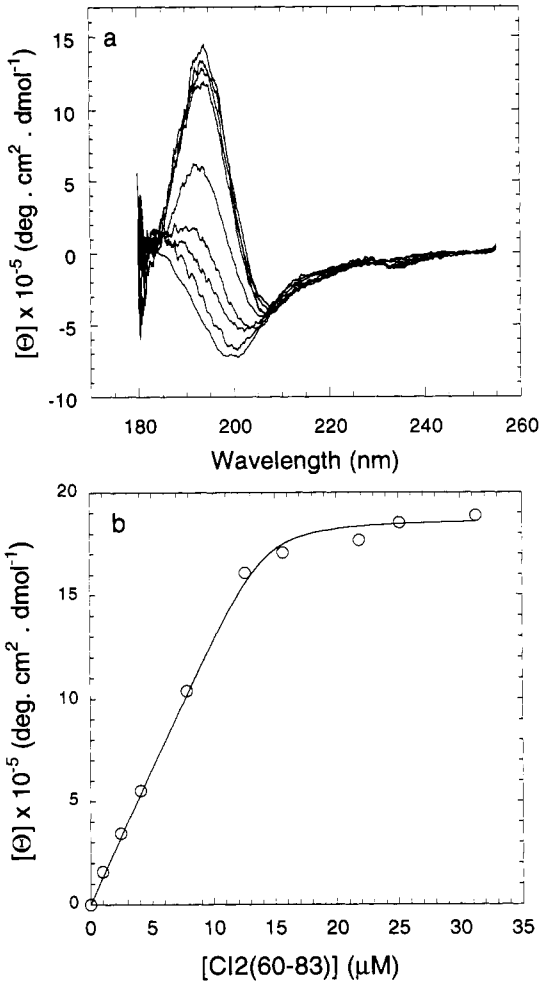

FIGURE 6: CD spectra obtained on the addition of CI-2(60–83) to CI-2(20–59). (a) 15 μM CI-2(20–59) was mixed with 0–30 μM CI-2(60–83) under the conditions described in Figure 5. At each concentration, the spectrum of CI-2(60–83) alone was subtracted, and the resultant spectra are represented in CI-2(20–59) molar based ellipticity. (b) The change in [Θ] at 193 nm from panel a is plotted against CI-2(60–83) concentration. The solid curve is the fit to eq 1, but the concentration was too high to obtain an accurate K_{diss} value.

monomer in the concentration range from 0 to 150 μM (not shown).

Tendency for α-Helix Formation of CI-2(20–59). The structure of full native CI-2 comprises the α-helix spanning residues 30–44. For studying the propensity of helix formation of the fragment CI-2(20–59), we recorded the far-UV circular dichroism spectra with and without the addition of TFE. CI-2(20–59) shows no presence of α-helix in water at 25 °C, but in the presence of 50% TFE the spectrum is typical of helical structure (not shown). On the other hand, in 5 M Gdm·Cl, the CD spectrum approaches the baseline, indicating the absence of defined structure. Using the method of Chen *et al.* (1972) and subtracting the contribution of random coil at 220 nm (Jasanoff & Fersht, 1994), we estimate 0% α-helix in 5 M Gdm·Cl, about 12% in water, and 42% in 50% TFE. The value in water is likely to be an overestimate since the assumptions of the method are for polypeptides where the α-helix has the larger contribution to the spectra. The far-UV spectrum of native uncleaved CI-2 does not show any significant contribution typical of α-helix, e.g., minima at 208 and 220 nm. Nevertheless, caution must be taken when α-helix properties are extrapolated from TFE to water (Zhong & Johnson, 1992; Sönnichsen, *et al.*, 1992).

^{1}H-NMR Spectra of Isolated Fragments and of the Complex. One-dimensional ^{1}H-NMR spectra of the two fragments are characteristic of a low extent of structure present, with a compressed pattern of peaks in the amide region (Figure 7a,b). The sharpness of the peaks suggests there is no irreversible aggregation or precipitation of the peptides in the experimental conditions used. A close analysis of CI-2(20–59) shows three peaks with chemical shifts of around 10 ppm which have been assigned to Trp-24 influenced by *cis–trans* isomerization of the adjacent Pro-25 (B. Davis, unpublished). Figure 7c shows that the complex regains much of the structure of native CI-2, as indicated by the dispersion of the peaks in the amide region, and also by the presence of chemical shifts at 10.9 and 11.7 ppm resembling the Glu-26 NH and Trp-24 indole N resonances observed in native uncleaved CI-2.

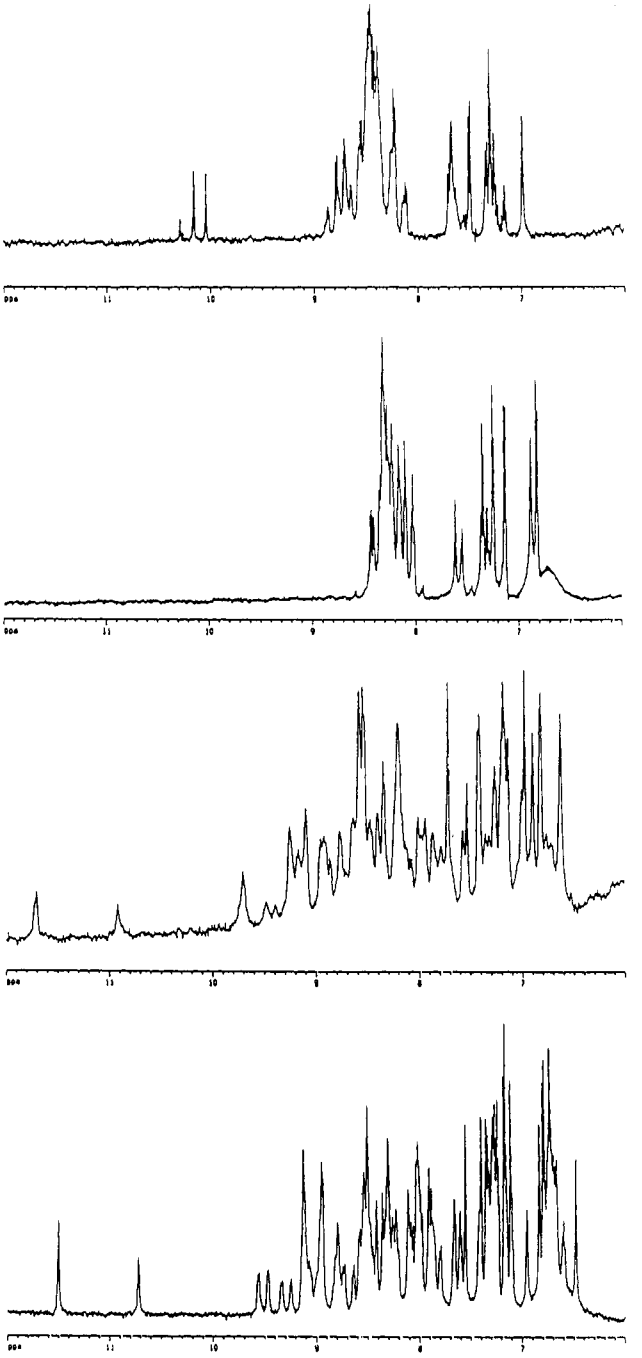

FIGURE 7: Amide region of one-dimensional ^{1}H-NMR of (a, top) CI-2(20–59), (b, second from top) CI-2(60–83), (c, second from bottom) [(20–59)·(60–83)], and (d, bottom) full CI-2. Protein concentration, 2 mM in panels a, b, and d and 0.6 mM in panel c. The samples were prepared as described in Materials and Methods, and the spectra were taken at 6 °C at pH 6.3.

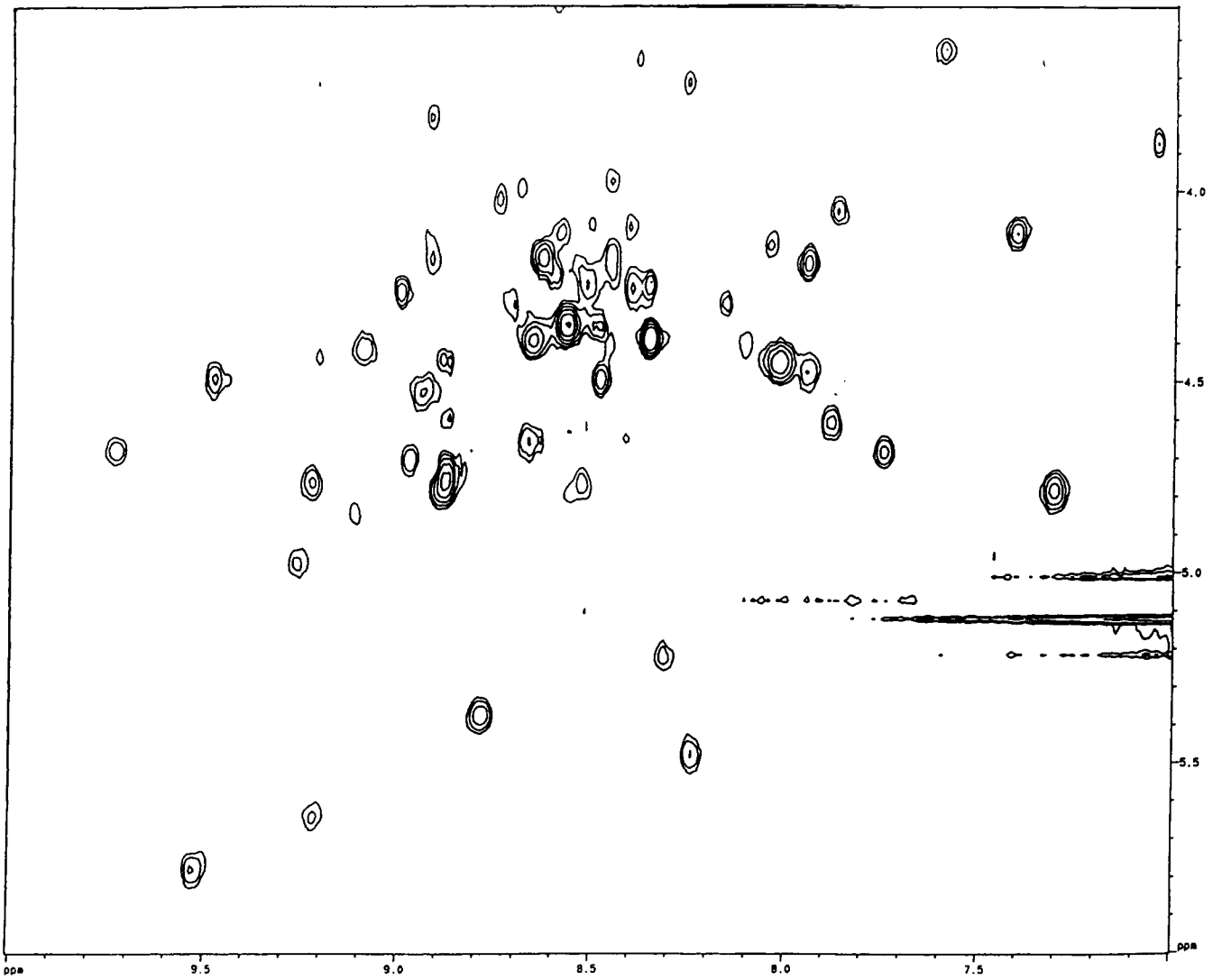

FIGURE 8: Expanded NH region of the two-dimensional ^{1}H-NMR NOESY spectrum of CI-2(20–59)·(60–83) complex. The protein concentration is 2.8 mM, at 50 mM acetate, pH 4.5, and 5 °C, in 90% H_2O/10% ^2H_2O.

The complex was also analyzed by two-dimensional NMR for further evidence of a folded structure. Figure 8 shows the amide (fingerprint) region of a 2D ^{1}H NOESY NMR spectrum, with several NOE cross peaks above the water, which is indicative of a folded structure. [CI-2(20–59)·(60–83)] complex was also analyzed by gel filtration on HPLC using a Superdex 75 column. The elution volume of the complex was 15.09 mL, compared with 15.15 mL of the uncleaved CI-2.

Protease Inhibitory Activity of the Complex [CI-2(20–59).(60–83)]. HPLC analysis showed that religation of the fragments does not occur even after three weeks of incubation of the complex (not shown). To test whether the cleaved reactive site (now HSer-59) is functional, we analyzed the inhibition capacity of [CI-2(20–59)·(60–83)] on α-chymotrypsin compared with uncleaved CI-2. Figure 9 shows that the complex is able to inhibit α-chymotrypsin, with an $[I]_{50\%}$ of 7 μM and 0.05 μM for uncleaved CI-2. The complex was analyzed by HPLC after the inhibition reaction (20 min) to verify that there was no degradation of the complex during the course of the reaction.

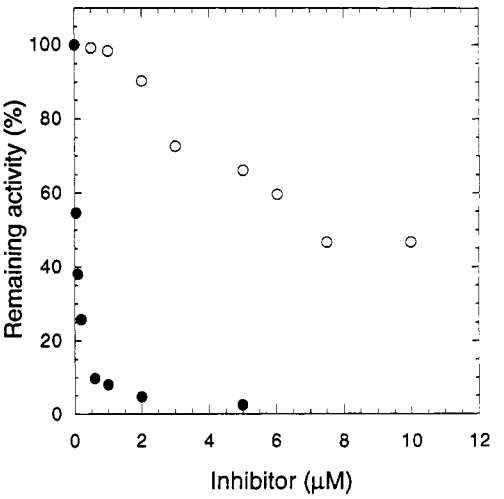

FIGURE 9: Inhibition of α-chymotrypsin by CI-2(20–59)·(60–83). The complex at each concentration was first formed and equilibrated for 1 h at 25 °C with Tris·HCl buffer, pH 8.6: intact CI-2 (●), fragments (○). Following a 20-min incubation with 50 nM α-chymotrypsin, the chromogenic substrate succinyl-Ala-Pro-Phe-*p*-nitroanilide was added to a final concentration of 1 mM, and the A_{420} change with time was recorded.

DISCUSSION

A naturally occurring chemical cleavage site in the loop of CI-2 has been selected to obtain two fragments, CI-2(20–59) and CI-2(60–83). Since the cleaved bond, Met-59–Glu-60, is located in the solvent-exposed reactive site loop (McPhalen & James, 1987), the strain induced in the structure should not be an obstacle for reassociation of the fragments. One of

the fragments, CI-2(20–59), contains a single Trp residue, allowing an easy monitoring of the process; similarly the fluorescence in native uncleaved CI-2 is much lower than that of the unfolded form (Jackson & Fersht, 1991). The fragments display a tight binding that could be measured at low concentration (0.5 μM); at high concentration, the isotherm for association titrates at 1:1 stoichiometry and the accurate determination of the binding constant is not possible. A similar behavior is observed when the same process is followed by ellipticity change at 15 μM concentration, indicating a cooperativity in the formation of tertiary and secondary structure. Fragment CI-2(20–59) is a monomer at the concentration range where the experiments were carried out.

The fragment CI-2(60–83) seems to have a highly disordered structure, as judged by CD and 1D NMR, but recent 2D NMR evidence from this laboratory indicates structure formation (B. Davis, in preparation). On the other hand, the shape of the CD spectra of the fragment CI-2(20–59) shows that there is residual structure present indicated by a shoulder at 212 nm and significant negative ellipticity around 220 nm; this is more evident when compared with the spectrum in Gdm·Cl (Figure 5b). In 50% TFE, CI-2(20–59) displays an α-helical structure, different from that found in the spectra of native intact CI-2. One-dimensional NMR spectra also suggest the presence of residual structure around Trp-24. The presence of structure in CI-2(20–59) is also being confirmed by two-dimensional NMR (B. Davis, in preparation).

The far-UV CD spectrum of the complex is identical to that of native uncleaved CI-2, strongly suggesting full recovery of the secondary structure. The change in the spectrum on formation of the complex with increasing concentration of CI-2(60–83) is dominated by the ellipticity change at 193 nm. The NMR experiments also support the formation of a folded structure, with a 2D NOESY spectrum showing a folded structure very similar to that of uncleaved CI-2 (B. Davis, unpublished). The complex can be denatured with Gdm·Cl, where the change is due to the dissociation-driven unfolding of [CI-2(20–59)·(60–83)] complex, which is completed at 2 M denaturant (Figure 3b). Temperature and pH studies also distinguish two states: folded complex and free fragments. However, the analysis made does not account for residual structure present in the fragments; they show neither fluorescence change in the range of Gdm·Cl where the complex dissociation/unfolding occurs nor significant transition in the thermodenaturation followed by CD.

Protein fragments may perhaps form structures that are relevant in early events in the folding pathway (Dyson *et al.*, 1992a). A similar observation was reported for an N-terminal fragment of barnase, which showed nascent helix structure similar to that of folded barnase (Sancho *et al.*, 1992). It has been shown for myohemerithrin, a four-helix bundle protein, that peptides spanning the different α-helical regions have propensity for preformed structures (Dyson *et al.*, 1992a). On the other hand, plastocyanin, largely a β-sheet protein, shows little tendency for preformed structures (Dyson *et al.*, 1992b). It needs to be confirmed whether the structure of CI-2(20–59) is similar to or different from the one in the native protein.

In this paper we described the association of two CI-2 fragments to give a structure highly similar to that of the uncleaved native protein. We also presented evidence that CI-2(20–59) is structured, whereas CI-2(60–83) is largely unstructured. In an accompanying paper (Prat Gay *et al.*, 1994) we present a detailed kinetic analysis and a possible mechanism of the association/complex folding of the two CI-2 fragments.

Many mutants of CI-2 have been constructed in this laboratory to study the mechanism of protein folding. The presence of Met-59 is common to all of these mutants, so the complementation studies described here may be extended to give a mutational analysis using both equilibrium and kinetic methods.

ACKNOWLEDGMENT

We thank Andrea Hounslow and Ben Davis for performing NMR experiments. Dr. P. J. G. Butler is gratefully acknowledged for the analytical centrifugation experiment. We also thank Dr. J. Ruiz-Sanz for helpful discussions.

REFERENCES

Anfinsen, C. B., & Scheraga, H. A. (1975) *Adv. Protein Chem. 29*, 205–300.
Brown, J. E., & Klee, W. A. (1971) *Biochemistry 10*, 470–476.
Butler, P. J. G., & Kühlbrandt, W. (1988) *Proc. Natl. Acad. Sci. U.S.A. 85*, 3797–3801.
Casassa, E. F., & Eisenberg, H. (1964) *Adv. Protein Chem. 19*, 287–395.
Chen, Y. H., Yang, J. T., & Martinez, H. M. (1972) *Biochemistry 11*, 4120–4131.
Clore, G. M., Gronenborn, A. M., Kjaer, M., & Poulsen, F. (1987) *Protein Eng. 1*, 305–311.
Dyson, H. J., & Wright, P. E. (1991) *Annu. Rev. Biophys. Chem. 20*, 519–538.
Dyson, H. J., Merutka, G., Waltho, J. P., Lerner, R. A., & Wright, P. E. (1992a) *J. Mol. Biol. 226*, 795–817.
Dyson, H. J., Sayre, J. R., Merutka, G., Shin, H-C., Lerner, R. A., & Wright, P. E. (1992b) *J. Mol. Biol. 226*, 819–835.
Gill, S. C., & von Hippel, P. H. (1989) *Anal. Biochem. 182*, 319–326.
Gross, E., & Witkop, B. (1961) *J. Am. Chem. Soc. 83*, 1510–1513.
Harpaz, Y., el Masry, N., Fersht, A. R., & Henrick, K. (1994) *Proc. Natl. Acad. Sci. U.S.A. 91*, 311–315.
Hartley, R. W. (1977) *J. Biol. Chem. 252*, 3252–3254.
Jackson, S. E., & Fersht, A. R. (1991) *Biochemistry 30*, 10428–10435.
Jackson, S. E., Moracci, M., el Masry, N., & Fersht, A. R. (1993) *Biochemistry 32*, 11261–11269.
Jasanoff, A., & Fersht, A. R. (1994) *Biochemistry 33*, 2129–2135.
Johnson, W. C., Jr. (1990) *Proteins: Struct., Funct., Genet. 7*, 205–214.
Longstaff, C., Campbell, A. F., & Fersht, A. R. (1990) *Biochemistry 29*, 7339–7347.
Ludvigsen, S., Shen, H., Kjaer, M., Madsen, J. C., & Poulsen, F. M. (1991) *J. Mol. Biol. 222*, 621–635.
McPhalen, C. A., & James, M. N. G. (1987) *Biochemistry 26*, 261–269.
Oas, T. G., & Kim, P. S. (1988) *Nature 336*, 42–48.
Prat Gay, G. de, Ruiz-Sanz, J., & Fersht, A. R. (1994) *Biochemistry* (following paper in this issue).
Saint Girons, I., Gilles, A. M., Margerita, D., Michelson, S., Monnot, M., Fermandjian, S., Danchin, A., & Bârzu, O. (1987) *J. Biol. Chem. 262*, 622–629.
Sancho, J., & Fersht, A. R. (1992) *J. Mol. Biol. 224*, 741–747.
Shiba, K., & Schimmel, P. (1992) *Proc. Natl. Acad. Sci. U.S.A. 89*, 1880–1884.
Sönnichsen, F. D., Van Eyk, J. E., Hodges, R. S., & Sykes, B. D. (1992) *Biochemistry 31*, 8790–8798.
Svendsen, I., Martin, B., & Jonassen, I. (1980) *Carlsberg Res. Commun. 45*, 79–85.
Tainuchi, H., & Anfinsen, C. B. (1971) *J. Biol. Chem. 246*, 2291–2296.
Tasayco, M. L., & Carey, J. (1992) *Science 255*, 594–597.
Zhong, L., & Johnson, W. C., Jr. (1992) *Proc. Natl. Acad. Sci. U.S.A. 89*, 4462–4465.